Reduced models of algae growth

Heikki Haario,[†] Leonid Kalachev[*] Marko Laine,[††]

† Lappeenranta University of Technology, Lappeenranta, Finland

∗ University of Montana, Missoula, MT, USA

†† Finnish Meteorological institute, Helsinki, Finland

Abstract

The simulation of biological systems often is plagued with a high noise level in the data as well as models loaded with a large number of correlated parameters. As a results, the parameters are poorly identified by the data and the reliability of the model predictions may remain questionable. Recently, the advance of Bayesian sampling methods has provided new methods for proper statistical analysis in such situations. Nevertheless, simulations should employ models that, on the one hand, are reduced as much as possible, and, on the other hand, are still able to capture the essential features of the phenomena studied. Here, in the case of algae growth modelling, we show how a systematic model reduction may be done. The simplified model is analyzed from both, theoretical and statistical, points of view.

Keywords: Algae growth modelling, asymptotic methods, model reduction, MCMC, Adaptive Markov chain Monte Carlo.

1 Introduction and motivation

Recent trends in the area of mathematical biology clearly indicate the shift from the, so-called, "soft modelling" that uses heuristical assumptions to produce qualitative results related to biological systems' behavior (usually without quantitative cross-validation of these results with real life data) to the, so-called, "hard modelling" where the model parameter values are obtained by fitting the model solutions to experimental data. The main goal of the latter approach is to produce quantitative description of the behavior of the biological systems. Such quantitative models are needed for making predictions for the future, especially, in cases where such predictions are closely related to potential human health hazards, or when they may have significant economic impact. The "hard modelling" approach is usually complicated by the fact that the available data coming from field measurements is very noisy and often incomplete, only some of the important variables can be measured, and the measurements, e.g., may not be uniform in space and time. For obtaining meaningful results, not only the parameter values must be found for such quantitative models, but also the reliability of the model predictions must be estimated. Running then "what if" scenarios based on the fitted models with various

choices of parameter values we may see what is "the best" and what is "the worst" that may happen in a given system. In statistical terms, this means that not only the best fitting parameter values are determined, but also the distribution of all possible parameter values is found, together with the distribution of model predictions. Here, we achieve this by employing Bayesian sampling methods.

We apply the "hard modelling" approach to analysis of a specific system, the blooming of algae in a lake. The practical goal is to find out whether certain measurements performed during the summer season may allow us to predict an explosion of poisonous algae population (or its absence) later in the summer. Knowledge of poisonous algae population dynamics could help to plan countermeasures (such as, e.g., restriction of lake use, increased fishing, etc.) ahead of time.

In the recent study [3] the confounded effects of nutrients and grazing zooplankton (Crustacea) on phytoplankton groups in a shallow, mesotrophic lake were estimated. The algae dynamics was modelled as a non-linear dynamic system which described the succession of three dominant algae groups (Diatomophyceae, Chrysophyceae, nitrogen-fixing Cyanobacteria) and minor groups summed together as functions of total phosphorus, total nitrogen, temperature, global irradiance and crustacean zooplankton grazing. The model was fitted using eight years of in situ observations and adaptive Markov chain Monte Carlo (MCMC) methods for estimation of model parameter distributions. This approach offered a way to deal with noisy data and a large number of weakly identifiable parameters in such a model. More details on the biological background and modelling issues may be found in [3].

While the statistical approach in [3] was shown to be successful, a high number of unknown, correlated parameters certainly implied difficulties: for parameter identification, one had to be able to set priors that, however, did not distort the estimation results. Also, the MCMC sampling schemes required long simulation runs, whose convergence was not easily verified. The reduction of the complexity of a model is an integral part of the modelling process. The resulting model should be as simple as possible, and still it must be supported by the available data. If the model is too complex, i.e., it contains too many parameters, some of these parameters will not be identifiable from the data. On the other hand, if the model is too simple, i.e., it contains too few parameters, the residual of the fit will be unacceptably large. Here we show how to reduce the algae model, so that it only contains two algae groups, without any essential loss in the prediction of the behavior of the most interesting group, Cyanobacteria. Simplification of the model greatly facilitates the statistical analysis of the situation, and also helps to perform a theoretical study of the transitions to possible steady states of the system.

2 Modelling and fit to data

In [3] the growth and decay mechanisms are integrated into a minimal mass-balance equation system for the wet weight concentration of algae. Here we review the main results of [3]. Phytoplankton is divided into four groups: Diatoms (A_1), Chrysophycea (A_2), nitrogen fixing Cyanobacteria (A_3), and several minor species summed together in

the fourth group (A_4). The biomass concentrations of A_i ($i = 1, \ldots, 4$) are denoted by C_{A_i} ([mg L^{-1}]), respectively. The model is given by the following system of ordinary differential equations

$$\frac{dC_{A_i}}{dt} = \left(\tilde{\mu}_i - \frac{\tilde{\sigma}_i}{h} - \frac{Q}{V} - p_i C_Z \right) C_{A_i}, \qquad i = 1, 2, 3, 4; \tag{1}$$

where the growth limiting factors and loss rates are given by

$$\begin{aligned} \tilde{\mu}_i &= \mu_i \theta_i^{T-T_{ref}} \frac{I}{K_{Ii} + I} \frac{P}{K_{Pi} + P} \frac{N}{K_{Ni} + N}, \\ \tilde{\sigma}_i &= \sigma_i \theta_\sigma^{T-T_{\mathrm{ref}}}. \end{aligned} \tag{2}$$

Here P and N denote the total amounts of phosphorus and nitrogen minus that included in the phytoplankton: $P = P_{\mathrm{tot}} - \sum_{i=1}^{4} \alpha_i C_{A_i}$ and $N = N_{\mathrm{tot}} - \sum_{i=1}^{4} \beta_i C_{A_i}$, where the constants α_i and β_i give the nutrition content of the corresponding phytoplankton species. The terms P_{tot} (total phosphorus), N_{tot} (total nitrogen), T (temperature), I (global irradiance), and C_Z (carbon mass concentration of zooplankton Z) are treated as control variables, given by measurements. The notations and roles of various variables and parameters are listed in Table 1.

Eight years of observations from the lake, collected between 1992 and 2000, were used for identifying the unknown parameters in the model. The observational error is modelled as a modified Gaussian distribution so as to take into account the heteroscedasticity and non-negativity of the data; see [3] for more details.

The values of the control variables are plotted, for all the years measured, in Figure 1.

Although the model itself is not complicated, we still have 8 parameters to be estimated for each of the four phytoplankton groups. Moreover, the four unknown initial algae concentration values for each of the eight summers must be considered. After a minor simplification (a common temperature coefficient for all the non–predatory losses, θ_σ) we are left with 61 model parameters to be estimated.

Without prior restrictions the parameters are clearly not identifiable by the measurements. However, it turned out that by using the priors available for several of the parameters, the parameter estimation could be carried out reasonably well. The statistical analysis for both the posterior distributions of the parameters and the model predictions was performed by extensive MCMC (Markov chain Monte Carlo) sampling methods. Table 2 gives the numerical values of the means and standard deviations as computed from the MCMC chain. Once again, for more details we refer the reader to [3].

Figure 2 shows the distributions of model predictions, obtained by calculating the model solutions for all the parameter values sampled from the parameter posterior distributions. Here we want to point out that the distributions of model predictions are reasonably narrow (if compared to quite high noise level of the data) even though many of the parameters are not well identified. This shows the power of the MCMC approach: it reveals the level of identification of the parameters, and simultaneously shows how much the possible non-uniqueness matters in terms of reliability of the model predictions. However, while it was possible to carry out the parameter identification for the full model, a

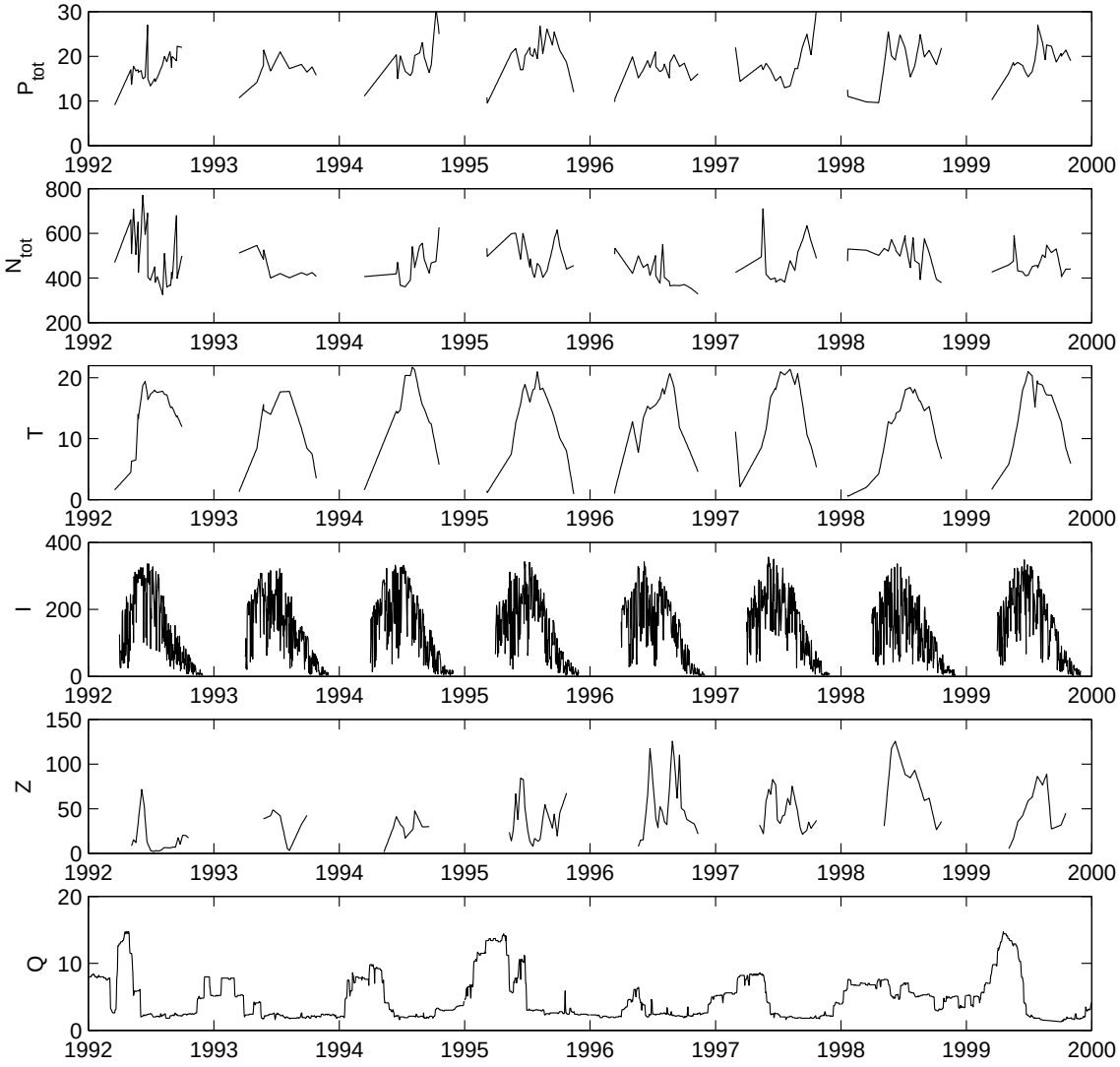

Figure 1: Time series of observed variables used in the algae model. Here P_{tot} is total phosphorus concentration [g L^{-1}], N_{tot} is total nitrogen concentration [g L^{-1}], T is water temperature [°C], I is global irradiance [W m^{-2}], Z is grazing zooplankton biomass concentration [g C L^{-1}], and Q is outflow rate [m^3s^{-1}].

Estimated parameters $i = 1, \ldots, 4$:

μ_i	maximum growth rate at 20 °C [d^{-1}]
σ_i	maximum non–predatory loss rate at 20 °C [md^{-1}]
θ_i, θ_σ	temperature coefficients for growth and non–predatory loss rate
K_{Ii}	global irradiance half-saturation coefficient [W m^{-2}]
K_{Pi}	phosphorus half-saturation coefficient [g L^{-1}]
K_{Ni}	nitrogen half-saturation coefficient [g L^{-1}]
p_i	zooplankton filtration rate [mgC L^{-1} d^{-1}]

Control variables:

P_{tot}	total phosphorus concentration [g L^{-1}]
N_{tot}	total nitrogen concentration [g L^{-1}]
C_Z	zooplankton herbivore (crustacea) carbon mass concentration [mgC L^{-1}]
T	temperature [°C]
Q	outflow [$\mathrm{m}^3\mathrm{s}^{-1}$]
I	global irradiance [W m^{-2}]

Known constants:

T_{ref}	the reference temperature (20 °C)
α_i	phosphorus content of A_i
β_i	nitrogen content of A_i
V	volume of lake [m^3]
h	depth of lake [m]

Table 1: Notations and units for the algae model parameters, data and constants.

considerable computational effort was required. In such a complex situation the sampling methods may need extensive 'tuning' before reasonable results are reached. In the present case, special adaptive methods were employed. Even so, quite long sampling chains had to be used. An obvious way to avoid such difficulties is to reduce the number of parameters to be estimated. The reductions should, however, be performed in such a way that the essential features of the model are preserved.

Below, we discuss the reduction in detail. The process consists of two parts: a structural reduction of the original model using asymptotic approach and further reduction of the number of model parameters of the already simplified model by MCMC runs.

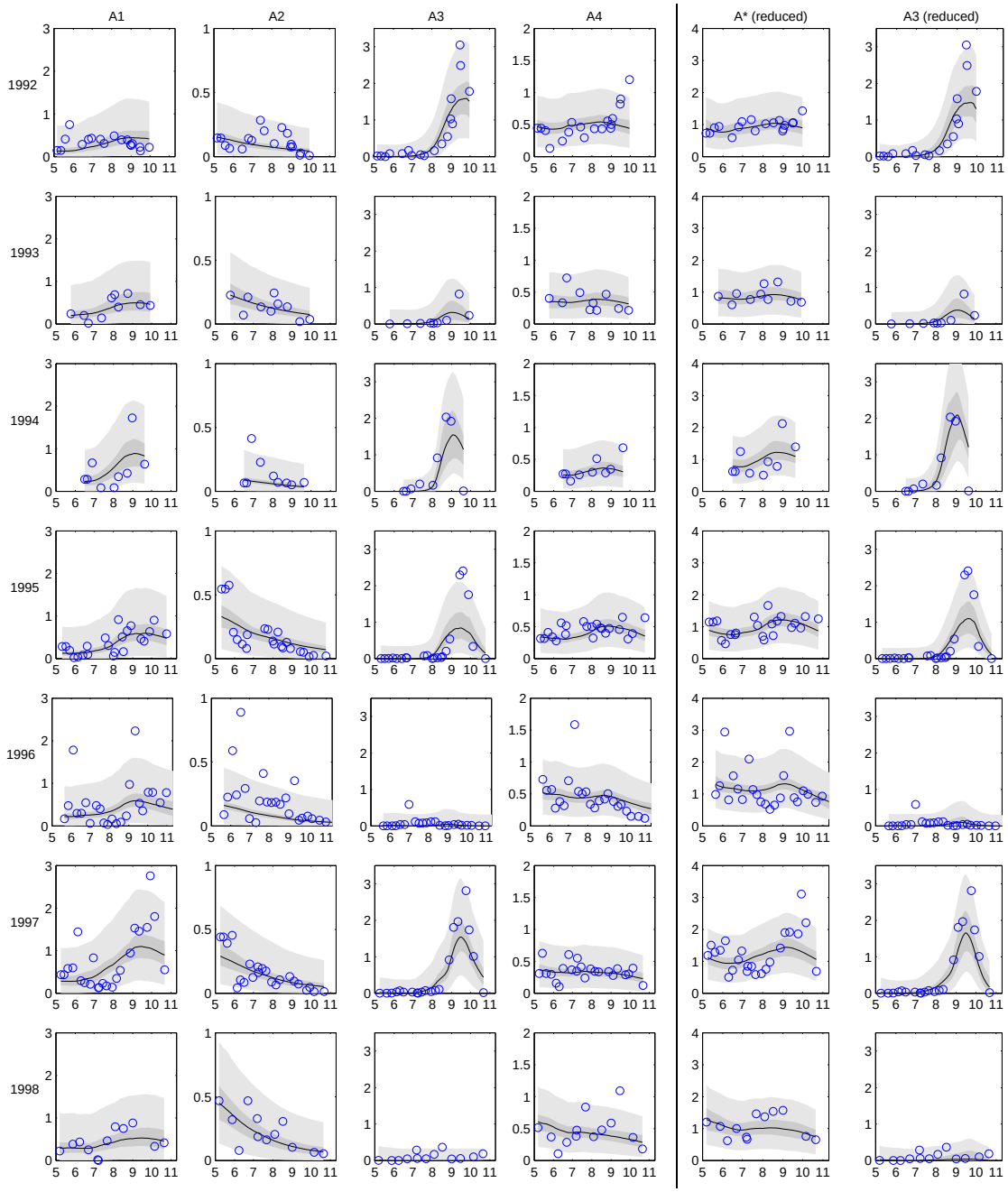

Figure 2: Plots of fitted models and uncertainties during the growing season. Circles (o) represent the observed algae wet biomass concentrations [mg L^{-1}]. Solid lines show the mean fits obtained by MCMC method. Darker areas correspond to 95% posterior limits of the model uncertainty, the lighter areas show uncertainty in predicting new observations. The horizontal axis shows months for the year. Columns 1–4 exhibit the results for the 4 algae model ([3]), the two rightmost columns present corresponding results computed with the reduced model.

	μ_i	σ_i	θ_i	K_I	K_P	K_N	p_i
1	0.0886 (0.043)	0.0845 0.062)	1.14 (0.051)	61.9 (48)	10.4 (5.3)	14.5 (11)	0.0438 (0.036)
2	0.0465 (0.033)	0.137 (0.077)	1.07 (0.049)	115 (60)	8.27 (4.9)	32.9 (22)	0.0665 (0.046)
3	0.329 (0.089)	0.349 (0.20)	1.16 (0.060)	16.4 (11)	5.50 (3.2)	21.0 (13)	1.09 (0.33)
4	0.212 (0.10)	0.0463 (0.025)	1.13 (0.051)	134 (67)	77.3 (28)	45.7 (28)	0.0802 (0.033)

Table 2: Posterior means and standard deviations (in parenthesis) of the estimated parameters of the phytoplankton model with 4 algae groups ([3]). Each row corresponds to the four algae groups. The common parameter for the temperature dependence of the loss rate, θ_σ, is not in the table. For this parameter we have corresponding values $\theta_\sigma = 1.05(0.060)$.

3 Model reduction

Here we show how, under certain conditions, the reduction of the 4 dimensional model presented earlier to a lower dimensional one can be done using asymptotic approach.

Let us assume that for some of the algae groups, A_i (in our case, $i = 1,\ 2,\ 4$), the coefficients in the equations have close numerical values. For example,

$$K_{I_i} = \bar{K}_I + \hat{K}_{I_i} \qquad \text{with} \quad \hat{K}_{I_i} \ll \bar{K}_I, \quad i = 1, 2, 4. \tag{3}$$

Then, we can write

$$K_{I_i} = \bar{K}_I \left(1 + \frac{\hat{K}_{I_i}}{\bar{K}_I}\right) = \bar{K}_I \left(1 + \epsilon \tilde{K}_{I_i}\right),$$

where $0 < \epsilon \ll 1$ is a small non-dimensional parameter, and non-dimensional coefficients $\tilde{K}_{I_i} = O(1)$ have moderate numerical values, so that the products $0 \ll \epsilon \tilde{K}_{I_i} \ll 1$ are numerically small.

We assume that all the other parameters in corresponding equations for A_i ($i = 1,\ 2,\ 4$) have representations similar to (3), e.g.,

$$K_{P_i} = \bar{K}_P \left(1 + \epsilon \tilde{K}_{P_i}\right), \quad K_{N_i} = \bar{K}_N \left(1 + \epsilon \tilde{K}_{N_i}\right), \quad \tilde{\mu}_i = \bar{\mu}\left(1 + \epsilon \tilde{\mu}_i\right), \quad \text{etc.} \tag{4}$$

A look at the values in Table 2 shows that the assumptions of type (3) are certainly true, e.g., for the parameters p_i describing the effect of zooplankton. Even if the situation is not as clear for some other parameters, we will see that the reduction still produces sufficiently accurate results. This is due to the fact that the posterior distributions of many of the parameters are quite wide (see the large posterior std values in that table).

Substituting (3), (4), and similar representations for other coefficients into the equations for concentrations C_{A_i} ($i = 1,\ 2,\ 4$), expanding coefficients into Taylor series with the center corresponding to $\epsilon = 0$, and collecting terms multiplying like powers of ϵ, we obtain:

$$\begin{aligned} \frac{dC_{A_i}}{dt} &= (\bar{\mu} - \bar{\sigma}/h - Q/V - \bar{p}C_Z)C_{A_i} \\ &+ \epsilon F_i(C_{A_1}, C_{A_2}, C_{A_3}, C_{A_4}, \tilde{\mu}, \tilde{K}_{I_i}, \tilde{K}_{P_i}, \tilde{K}_{N_i}, \ldots) + \ldots, \\ &\quad i = 1, 2, 4. \end{aligned} \tag{5}$$

Here F_i are known functions of the parameters and C_{A_i}; higher order terms in ϵ (not shown in (5)) depend on ϵ^2, ϵ^3, etc.

Let us look for concentrations C_{A_i} ($i = 1,\ 2,\ 4$) also in form of the expansions:

$$C_{A_i} = \bar{C}_{A_i} + \epsilon \tilde{C}_{A_i} + \ldots. \tag{6}$$

Substituting (6) into (5), and setting $\epsilon = 0$, we obtain the equations for the leading order approximations of corresponding concentrations:

$$\begin{aligned} \frac{d\bar{C}_{A_i}}{dt} &= (\bar{\mu} - \bar{\sigma}/h - Q/V - \bar{p}C_Z)\bar{C}_{A_i}, \\ & \\ & i = 1, 2, 4. \end{aligned} \tag{7}$$

We note that we can now add the tree equations of (7) to obtain:

$$\frac{dC_A^*}{dt} = (\bar{\mu} - \bar{\sigma}/h - Q/V - \bar{p}C_Z)C_A^*, \tag{8}$$

where

$$C_A^* = \bar{C}_{A_1} + \bar{C}_{A_2} + \bar{C}_{A_4}.$$

Thus, instead of the original 4 dimensional model we can now study a two dimensional reduced model for C_A^* and C_{A_3}:

$$\begin{aligned} \frac{dC_A^*}{dt} &= (\bar{\mu} - \bar{\sigma}/h - Q/V - \bar{p}C_Z)\bar{C}_A^*, \\ \frac{dC_{A_3}}{dt} &= (\mu_3 - \sigma_3/h - Q/V - p_3C_Z)C_{A_3}, \end{aligned} \tag{9}$$

where, e.g.,

$$\bar{\mu} = \bar{\mu}^*\bar{\mu}(T)\frac{I}{\bar{K}_I + I}\frac{P}{\bar{K}_P + P}\frac{N}{\bar{K}_N + N}$$

$$\tilde{\mu}_3 = \mu_3^*\mu_3(T)\frac{I}{K_{I_3} + I}\frac{P}{K_{P_3} + P}\frac{N}{K_{N_3} + N}$$

with

$$\bar{\mu} = \bar{\theta}^{(T-T_{ref})}, \qquad \mu_3 = \theta_3^{(T-T_{ref})},$$

$$P = P_{tot} - \bar{\alpha}C_A^* - \alpha_3C_{A_3}, \quad N = N_{tot} - \bar{\beta}C_A^* - \beta_3C_{A_3}, \quad \text{etc.}$$

This means that in the leading order approximation we may only consider "two species": A_3 and $A^* = A_1 + A_2 + A_3$. Differentiation in the species dynamics for A_1, A_2, A_3 occurs only in the higher order approximations.

For the above asymptotic reduction procedure to work the viability of assumptions (3) – (4), etc., must be checked for the time intervals of interest.

4 Results for the reduced model

In principle, in the cases where the characteristic values of coefficients for various species in the model are not known beforehand, the fit for the full model may be done first. Then, if the pattern could be established in fitted parameter values indicating that for some species respective coefficients are of the same order of magnitude (or they have close

numerical values), the reduction of the full model to a smaller dimensional one can be performed, and the results given by the two models may be compared.

For the present case, the results of such a comparison were created: a parameter vector (of dimension 61) from the posterior distribution of the original model was selected and the model predictions were calculated. New predictions for the reduced model were then computed by substituting respective mean values of parameters and new initial values into the reduced ODE model (9). In Figure 3 we present the comparison of computed solutions describing Cyanobacteria for the original and the reduced model. We see that the results obtained by the reduced model for the Cyanobacteria algae are close to those of the original model. Indeed, they are clearly inside the statistical variability presented in Figure 2.

Next, we once again analyze the parameters (now 31 instead of 61) of the reduced model. The parameter distributions of the reduced model are studied by MCMC sampling just as with the original model. Only the sampling is easier to perform, since the number of the parameters is reduced to one half of that of the original.

In Table 3 we presen the initial values of the parameters together with the respective priors used for the first MCMC run performed with the reduced model. For some of the parameters, especially the temperature coefficients θ_i, reasonably accurate priors may be used, while for the rest of the parameters we essentially employ lower and upper bounds only. For the initial concentrations of algae groups at the beginning of each summer season we used Gaussian priors with center points and variances estimated by the data.

parameter	*prior mean / initial value*	*prior std*	*posterior mean*	*posterior std*
μ_1	0.100	∞	0.623	0.32
μ_3	0.329	∞	0.485	0.15
σ_1	0.015	∞	0.138	0.060
σ_3	0.317	∞	0.640	0.21
θ_1	1.07	0.08	1.14	0.054
θ_3	1.16	0.08	1.14	0.046
θ_σ	1.20	0.09	1.04	0.048
K_{I1}	100	100	.	.
K_{I3}	100	100	.	.
K_{P1}	10	20	.	.
K_{P3}	10	20	10.1	6.3
K_{N1}	10	40	7990	4900
K_{N3}	10	20	.	.
p_1	0.07	∞	.	.
p_3	1.09	∞	1.15	0.36

Table 3: Ininital and prior values for the reduced model. The prior for the initial concentration at the beginning of the summer was normally distributed, $N(1, 0.6^2)$, for the combined group and $N(0.0001, 0.02^2)$ for the cyanobacteria. Additional positivity constraint was set for all of the unknowns.

After an initial LSQ fit of the parameters, a chain of length 500 000 was sampled using the Delayed rejection - Adaptive Metropolis (DRAM) algorithm ([6]). The Figure (4) presents 1D marginal posterior distributions produced by the MCMC run for the reduced model. We see that several of the parameters take values close to zero. The half saturation parameters $K_{I1}, K_{I3}, K_{P1}, K_{N3}$ all appear as denominators of the respective Monod terms, which, thus, may be replaced by the constant value 1. In addition, the zooplankton grazing term p_1 may be set to zero.

A new fit together with the ensuing MCMC sampling was performed for the model further reduced. Now the model contains 26 parameters, including 16 initial conditions. Figure (5) shows the histograms distributions of the parametetrs produced by the final MCMC run. Figure (6) presents the 1D and 2D marginal posterior distributions of the parameters $\mu_3, \sigma_3, \theta_3, K_{P3}, p_3$ of the Cyanobacteria group.

To create the distributions for the algae concentrations, the respective model responses were saved (at each 100'th sample, so as to minimize the size of the output files and to select non-correlated samples). At each time point, the histograms of the model values were then created. The resulting distributions for the Cyanobacteria responses are shown in Figure 2, in two rightmost columns. We can see that the outcome is essentially the same as that calculated in [3] using the full model with four algae groups.

Inevitably, some features of the original model are lost in the reduction. In particular, note the slightly increasing and decreasing trends of algae groups 1 and 2 in Figure 2, two leftmost columns. The addition of the measurements of the three combined groups leads to data that might be characterized as background noise. Indeed, the role of this pooled group in the model mainly is to provide nutrient competition for Cyanobacteria. We would like to mention that modelling the Cyanobacteria dynamics using a model that only contains that one algae group did not lead to a satisfactory result.

5 Numerical results for the long–time behavior of the reduced model

In Appendix A we present the analysis of the autonomous version of model system (9). There we analyze the steady states of this system as well as their stability properties. In Appendix B we prove that there is at most one co-existence steady state of (9) for which both populations concentrations, C_A^* and C_{A_3}, are non-zero. The analysis shows that an analog of the classical *principle of competitive exclusion* (see, e.g., Murray [7]) is observed for this system. For various parameter values and different initial conditions either one population or the other goes extinct. There also exists a set of parameter values for which both populations may co-exist.

To specify model predictions for future time values we must determine how to choose the model variables: the initial states, the estimated parameters, and the control variables. With any fixed values of these, the prediction is a straightforward integration of the ODE system for the model. But for a realistic evaluation of the predictions, we would like to add the uncertainties for each of the variables, and create the distributions of the

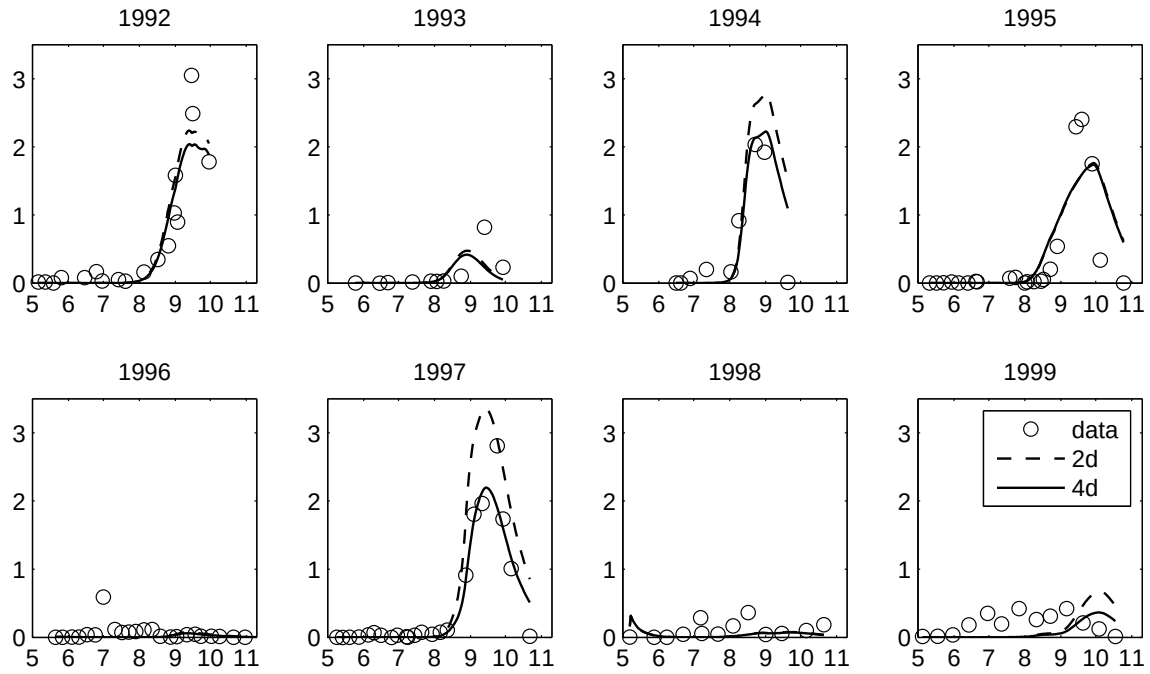

Figure 3: Example plots for predictions of Cyanobacteria produced by the full model (solid line) and by corresponding reduced model (broken line). Circles (o) represent the observed Cyanobacteria algae wet biomass concentrations [mg L^{-1}]. The horizontal axis shows months of the year.

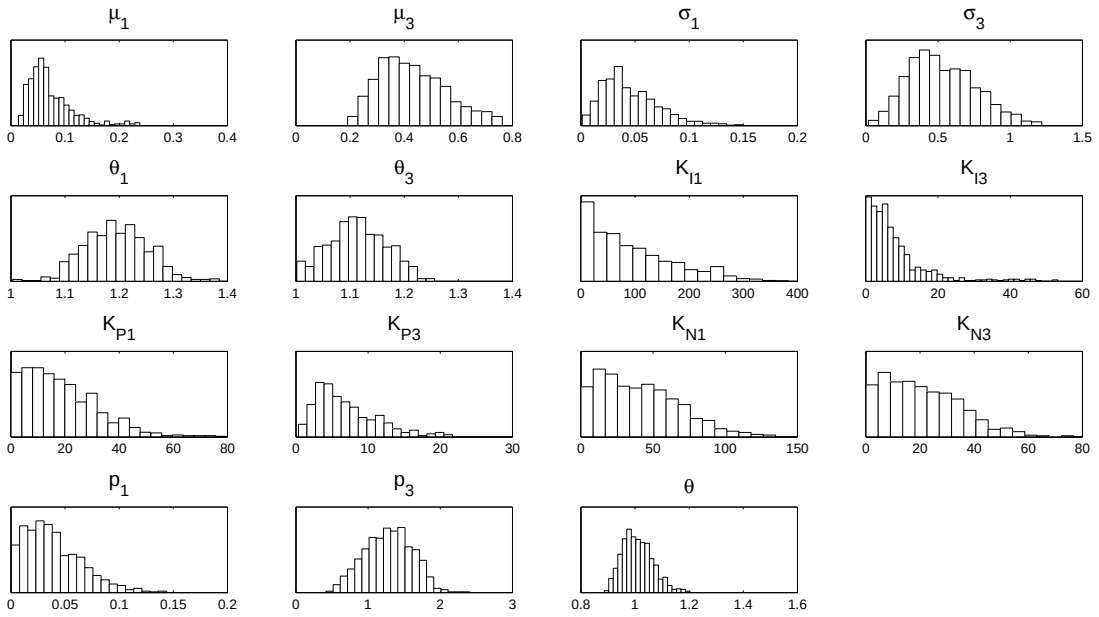

Figure 4: Histograms of the parameters of the reduced model as produced by the MCMC chain.

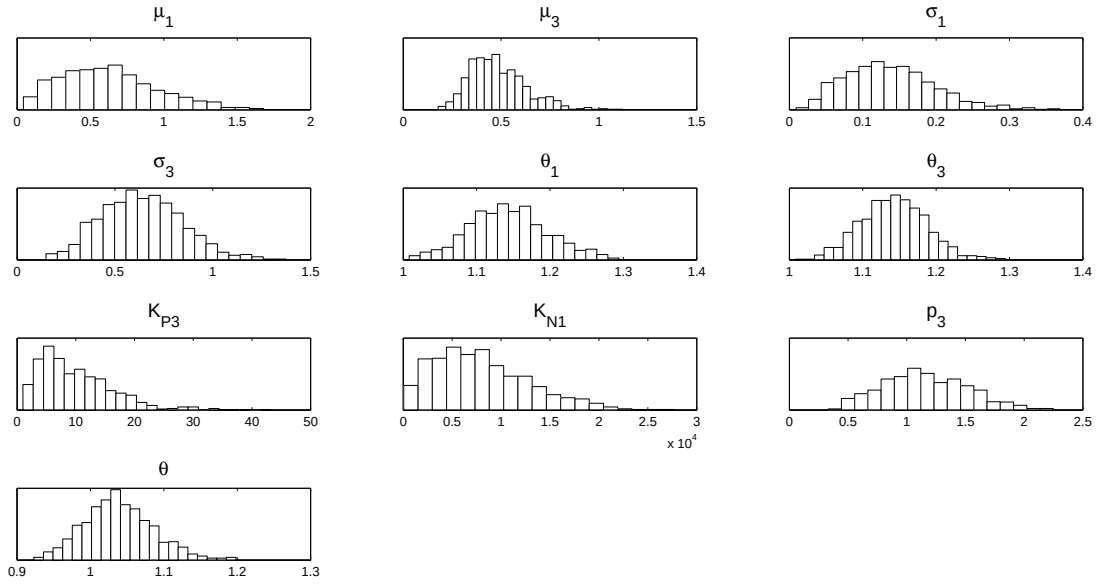

Figure 5: Histograms of the parameters of the reduced parameter set of as produced by the MCMC chain.

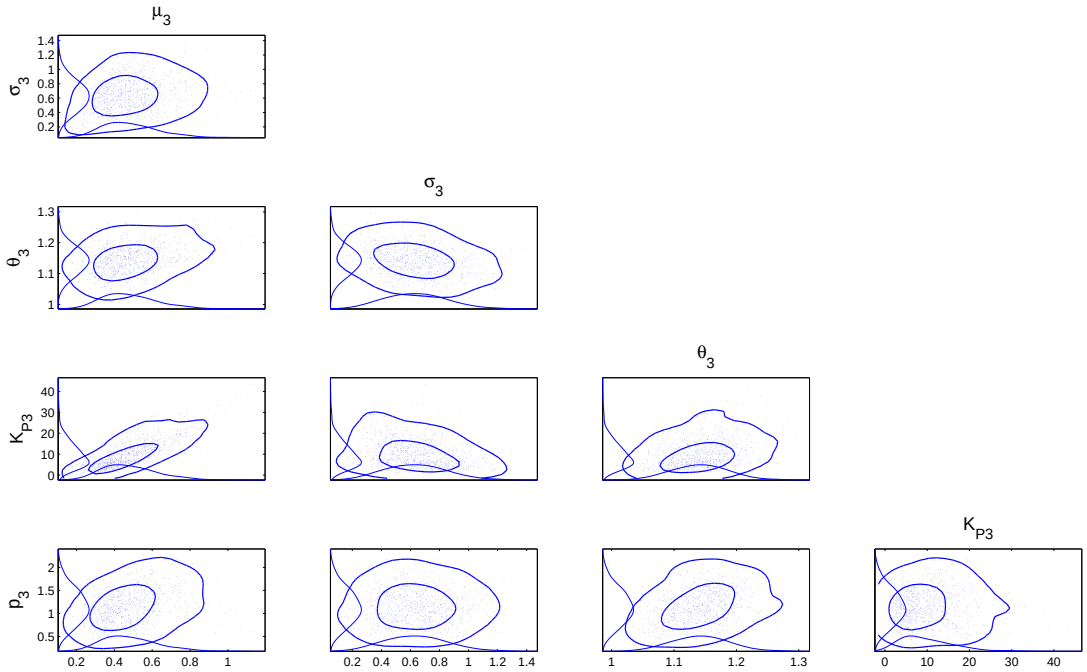

Figure 6: 2D and 1D marginal posterior distributions for the reduced parameter set of the Cyanobacteria group.

predictions instead of unique prediction curves. For the parameter values the procedure is clear: we sample parameter vectors from the posterior distribution (the MCMC chain previously created) and calculate the model prediction for each sampled vector. Similarly, we may sample the initial algae concentrations from the respective posterior distributions – we note that the true state of a lake is never accurately known. The situation with the control variables is somewhat more problematic: the values used in the calibration are based on measurements, but no such values may exist in the future. So, we must be satisfied with some average or typical values, or resort to the 'what if' scenarios, to calculate the behavior of the system with, e.g., extremal yet realistic values. Naturally, for short term predictions, plausible estimates for the temperature or nutrients may be available.

Below, a few examples of the long–term behavior of the model are presented. 'Typical' values of the control variables P_{tot} (total phosphorus concentration), T (water temperature), C_Z (grazing zooplankton biomass concentration), N_{tot} (total nitrogen concentration) and Q (outflow rate) were used. These profiles were created by choosing the minimal and maximal values of the respective variables from all the data available, separately for each time point during the summer, and computing then the mean values. Keeping the control variables fixed to these profiles, we calculated the model prediction distributions by sampling the initial states and model parameter values from the MCMC chains.

For the transition to steady state analysis, we want to see the behavior of the model in cases were all the control variables are fixed to a constant value, and the integration

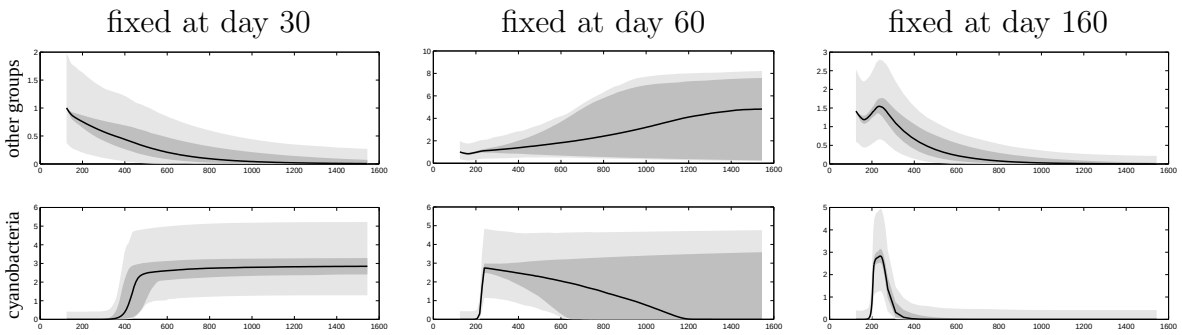

Figure 7: Examples of the dynamics for carrying capacity: long term behavior of the model with all the control parameters fixed after a given date. The algae wet biomass concentrations are simulated with various paraeter combinations sampled from the parameter posterior distribution. The gray areas correspond to posterior 95% probability regions of predicted mean algae biomass (darker) and of predicted future observation (lighter gray). Vertical axis has algae concentration [mg L^{-1}], horizontal axis has days.

is continued for large times. The parameter values are sampled as above. Figure 7 gives the prediction distributions for three different situations, were the control variables are 'frozen' in early summer, July and August, respectively. We see that the theoretically possible steady–states do occur: the trivial steady state where both of the groups vanish appears in the late-summer conditions, while one of the groups prevail in the early and mid-summer situations. Note that the spread of possible outcomes is large in the mid-summer situation. Depending on the parameters and initial values, either one of the groups may take over. This specific situation is further illustrated by the phase-plane plot in Figure 8. Here, the circles close to the x–axis near the origin denote the initial values, while the squares, stars and diamonds denote states of the system at a large time point. Note that most of the final states are on the x–axis or y–axis, representing cases where one of the two groups has taken over. However, some of the final states show that both groups still co-exist at a large time point. Those situations exemplify the steady-state with both species populations being non-zero, or a situation close to it, i.e., a very slow convergence towards a one-group steady state. We also note that for the case of day 60 (midsummer) conditions the increase of the Cyanobacteria concentrations is quite rapid, while the dynamics of the system in the other situations is considerably slower.

6 Conclusion

We presented a reduced model of algae growth consisting of 2 differential equations and compared its behavior with that of the original model containing 4 differential equations. Both models were fitted to available data and reliability regions for parameter estimates were constructed using the MCMC approach.

The model simplification was successful, the reduction to two algae groups did not

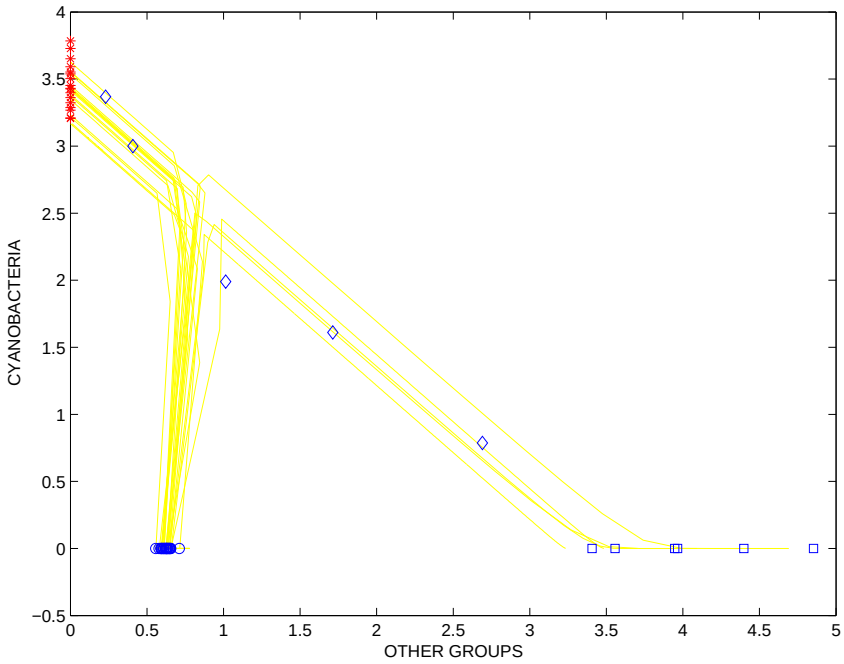

Figure 8: A phase space example of the long-term behavior of the model with all the control parameters fixed after a given date. The trajectories corresponds to the case "fixed at day 60" shown in Figure 7. The algae wet biomass concentrations of the two groups [mg L^{-1}] are plotted against each other. They are calculated using various parameter combinations sampled from the parameter posterior distribution. The circles denote the starting values. The steady state values where Cyanobacteria prevails are marked with stars on the Y-axis. The steady states for which other groups prevail are marked with squares. Diamonds mark the situation where both groups survived for long times.

affect the predictive distribution statistics for the Cyanobacteria behavior. On the one hand, this means that the original model with four groups (and 61 parameters) contains a large number of redundant factors and parameters. It is remarkable, that it was possible to successfully perform the sampling even in such an overparametrized situation with highly noisy data. This may be seen as an example of the strength of the MCMC approach. On the other hand, it certainly pays off to reduce the models as much as possible: the MCMC runs were clearly easier to perform with the reduced number of parameters in the simplified model. Indeed, very long (typically of length 1000 000) sampling chains were needed for obtaining reliable results in the four algae case, while much shorter (of order 100 000) sampling chains were sufficient for the reduced model. The use of adaptive sampling schemes ([4], [6], [3]) greatly reduces the need for manual 'tuning' of the sampling schemes. Even so, in complicated situations similar to the one presented in this paper, one typically tends to repeat the MCMC runs or continue a previous run with a new one. The amount of this additional work, too, is considerably smaller for the case when a reduced model is used.

A theoretical study on the possible steady states of the model with fixed control factor values was performed. All the qualitatively different steady state situations (0,1, or 2 species alive) may theoretically occur. Numerical examples, calculated with samples from parameter distributions created, show that all the possible steady states do, indeed, occur.

While no steady state might truly exists in nature, the study of the transients towards the steady states of the model under different conditions gives us an insight to the dynamics of the system: sometimes the algae blooming may occur quite fast, while the system typically decays very slowly towards a steady state, see Figure (7).

Realistic predictions of the algae dynamics may be produced for various 'what if' scenarios by creating different profiles for the control variables. By the MCMC approach, such analysis may be supplied with proper distributions for the predictions. Thus, we are able to estimate the reliability of the predictions: under certain conditions all the sampled predictions point to essentially the same near-future behavior, while other conditions (near the boundaries of the domains of attractions of the system, together with the uncertainty in the parameter values as well as in the initial state values) would lead to considerable spread of the predictions.

References

[1] Haario H., Kalachev L., Lehtonen J., Salmi T. *Asymptotic Analysis of Chemical reactions*. Chem. Eng. Sci. Vol. 54, pp. 1131–1143, 1999.

[2] A.B. Vasil'eva, A.B. Butuzov and L.V. Kalachev: *The Boundary Function Method for Singular Perturbation Problems*, Philadelphia: SIAM, 1995.

[3] O. Malve, M. Laine, H. Haario, T. Kirkkala, J. Sarvala: *Bayesian modelling of algal mass occurrences – using adaptive MCMC methods with a lake water quality model*, Environmental Modelling & Software, 7(22):966–977, 2007.

[4] H. Haario, E. Saksman, and J. Tamminen. An adaptive Metropolis algorithm. *Bernoulli*, 7(2):223–242, 2001.

[5] H. Haario, M. Laine, M. Lehtinen, E. Saksman, and J. Tamminen. MCMC methods for high dimensional inversion in remote sensing. *Journal of the Royal Statistical Society, Series B*, 66(3):591–607, 2004.

[6] H. Haario, M. Laine, A. Mira, and E. Saksman. DRAM: Efficient adaptive MCMC. *Statistics and Computing*, 16:339–354, 2006.

[7] J.D. Murray, Mathematical Biology, Springer-Verlag, New York - Berlin - Heidelberg, 1993.

Appendix A. Reduced model analysis: steady states, their existence and stability

Here we discuss the long–term behavior of the system derived in Section 3. We start with introducing somewhat simplified notation. Below we write the equations for phytoplankton population concentrations, $C_1 = C_{A^*}$ and $C_2 = C_{A_3}$. In these equations we omit over bars in the notations for coefficients, we also introduce corresponding numerical sub- and super-indices; the meaning of new simplified notations is immediately clear from comparison with (9). The system now has the form:

$$\frac{dC_i}{dt} = \left[\mu_i - \frac{\sigma_i}{h_i} - \frac{Q}{V} - p_i C_Z\right] C_i, \quad i = 1, 2; \tag{10}$$

where

$$\mu_i = \mu_i^* \theta_i^{T-T_{ref}} \frac{P}{(K_1^i + P)} \frac{N}{(K_2^i + N)} \frac{I}{(K_3^i + I)},$$

$$\sigma_i = \sigma_i^* \theta_\sigma^{T-T_{ref}}.$$

Equations (10) are supplied with initial conditions

$$C_i(0) = C_i^*. \tag{11}$$

We note that total phosphorous $P_{tot}(t)$ and total nitrogen $N_{tot}(t)$ are measured experimentally. If we denote the phosphorous content of the two types of phytoplankton by α_i, and corresponding nitrogen content by β_i, respectively, then

$$P(t) = P_{tot} - \alpha_1 C_1(t) - \alpha_2 C_2(t), \qquad N(t) = N_{tot} - \beta_1 C_1(t) - \beta_2 C_2(t). \tag{12}$$

Substituting (12) into (10), we obtain:

$$\frac{dC_i}{dt} = \left[\mu_i(t)\frac{P_{tot}-\alpha_1 C_1-\alpha_2 C_2}{(K_1^i+P_{tot}-\alpha_1 C_1-\alpha_2 C_2)}\frac{N_{tot}-\beta_1 C_1-\beta_2 C_2}{(K_2^i+N_{tot}-\beta_1 C_1-\beta_2 C_2)}-M_i(t)\right]C_i. \tag{13}$$

Here we used notation

$$M_i(t)=\frac{\sigma_i}{h_i}+\frac{Q}{V}+p_i C_Z,$$

$$\mu_i(t)=\mu_i(T,I)=\mu_i^*\theta_i^{T-T_{ref}}\frac{I}{(K_3^i+I)}$$

to *clarify the structure* of the equations (compare with (1), (2), and (9)).

The concepts of *carrying capacity* and *competitive exclusion vs. co-existence* are naturally defined for autonomous (i.e., right hand side does not depend on time variable explicitly) differential equation models in ecology. Let us explain how these concepts can be extended to the model written above. Essentially, we want to show that possible steady states are their stability properties are qualitatively similar to those usually defined for classical *competition models*. The main difference will be in the fact that for classical case the null-clines are linear functions, while here the null-clines are represented by nonlinear functions, and thus, e.g., the proof of the uniqueness of a possible co-existence steady state solution is more complex.

Let us consider an autonomous version of (13) that we re-write in the form:

$$\begin{aligned}\frac{dC_1}{dt} &= F_1(C_1,C_2)\equiv G_1(C_1,C_2)\cdot C_1,\\ \frac{dC_2}{dt} &= F_2(C_1,C_2)\equiv G_2(C_1,C_2)\cdot C_2.\end{aligned} \tag{14}$$

Here F_i $(i=1,2)$ are the autonomous right-hand sides of the two equations in (13), and

$$G_i(C_1,C_2) = \left[\mu_i\frac{P_{tot}-\alpha_1 C_1-\alpha_2 C_2}{(K_1^i+P_{tot}-\alpha_1 C_1-\alpha_2 C_2)}\frac{N_{tot}-\beta_1 C_1-\beta_2 C_2}{(K_2^i+N_{tot}-\beta_1 C_1-\beta_2 C_2)}-M_i\right], \tag{15}$$
$$(i=1,2),$$

where we assume that μ_i, P_{tot}, N_{tot}, M_i, etc., are all constants.

The steady states $(\bar{C}_1,\bar{C}_2)$ of (14) are found as simultaneous solutions of the equations:

$$F_1(C_1,C_2)=G_1(C_1,C_2)C_1=0, \qquad F_2(C_1,C_2)=G_1(C_2,C_2)C_2=0. \tag{16}$$

Stability properties of the steady states are related to the signs of the real parts of the eigenvalues of the Jacobian matrix computed from (14) and evaluated at these steady states: for stability all real parts must be negative. The Jacobian matrix has the form:

$$J(C_1,C_2)=\begin{pmatrix} \dfrac{\partial F_1}{\partial C_1}(C_1,C_2) & \dfrac{\partial F_1}{\partial C_2}(C_1,C_2) \\ \dfrac{\partial F_2}{\partial C_1}(C_1,C_2) & \dfrac{\partial F_2}{\partial C_2}(C_1,C_2) \end{pmatrix}$$
$$=\begin{pmatrix} \dfrac{\partial G_1}{\partial C_1}\cdot C_1+G_1(C_1,C_2) & \dfrac{\partial G_1}{\partial C_2}\cdot C_1 \\ \dfrac{\partial G_2}{\partial C_1}\cdot C_2 & \dfrac{\partial G_2}{\partial C_2}\cdot C_2+G_2(C_1,C_2) \end{pmatrix}. \tag{17}$$

Obviously, one of the equilibrium solutions of (16) is trivial:

$$\bar{C}_1=0,\quad \bar{C}_2=0. \tag{18}$$

It always exists.

Jacobian matrix evaluated on this steady state has the following structure:

$$J(0,0)=\begin{pmatrix} G_1(0,0) & 0 \\ 0 & G_2(0,0) \end{pmatrix}. \tag{19}$$

For stability of this trivial equilibrium solution the following conditions must be satisfied that guarantee that the real eigenvalues, λ_i $(i=1,2)$, of $J(0,0)$ are negative:

$$\lambda_i=G_i(0,0)=\left[\mu_i\frac{P_{tot}}{(K_1^i+P_{tot})}\frac{N_{tot}}{(K_2^i+N_{tot})}-M_i\right]<0. \tag{20}$$

Since, as can be easily seen, $G_i(C_1,C_2)<G_i(0,0)$ $(i=1,2)$ for biologically meaningful values of $C_1>0$, $C_2>0$, we have that when the stability conditions for the trivial steady state are satisfied, no other non-trivial steady states can exist. As we show below, the conditions leading to appearance of the non-trivial steady states are equivalent to violation of at least one of conditions (20): the trivial steady state becomes unstable when non-trivial steady state(s) emerge.

Two additional steady state solutions can be obtained by setting one of the variables in (16) to zero. Let us, e.g., consider $\bar{C}_2=0$ (the case $\bar{C}_1=0$ is analyzed in a similar way). Then $C_1=\bar{C}_1>0$ must be a solution of the following equation:

$$G_1(C_1,0)=\left[\mu_1\frac{P_{tot}-\alpha_1C_1}{(K_1^1+P_{tot}-\alpha_1C_1)}\frac{N_{tot}-\beta_1C_1}{(K_2^1+N_{tot}-\beta_1C_1)}-M_1\right]=0. \tag{21}$$

The Jacobian matrix evaluated on this steady state solution will have the form:

$$J(\bar{C}_1,0)=\begin{pmatrix} \dfrac{\partial G_1}{\partial C_1}(\bar{C}_1,0)\cdot\bar{C}_1 & \dfrac{\partial G_1}{\partial C_2}(\bar{C}_1,0)\cdot\bar{C}_1 \\ 0 & G_2(\bar{C}_1,0) \end{pmatrix}. \tag{22}$$

For stability of this steady state we must have:

$$\lambda_1 = \frac{\partial G_1}{\partial C_1}(\bar{C}_1, 0) \cdot \bar{C}_1 < 0,$$
$$\lambda_2 = G_2(\bar{C}_1, 0) < 0. \tag{23}$$

Let us show that, when this is the only non-trivial steady state, the sufficient conditions that guarantee the existence of this steady state are also the conditions for its stability. Let us assume that

$$G_1(0,0) = \left[\mu_1 \frac{P_{tot}}{(K_1^1 + P_{tot})} \frac{N_{tot}}{(K_2^1 + N_{tot})} - M_1\right] > 0, \tag{24}$$

and

$$G_2(0,0) = \left[\mu_2 \frac{P_{tot}}{(K_1^2 + P_{tot})} \frac{N_{tot}}{(K_2^2 + N_{tot})} - M_2\right] < 0. \tag{25}$$

Then the second stability condition, on λ_2, in (23) is satisfied since $G_2(\bar{C}_1, 0) < G_2(0,0)$ for biologically meaningful $\bar{C}_1 > 0$ belonging to the interval $(0, \min[P_{tot}/\alpha_1, N_{tot}/\beta_1])$. For any $\bar{C}_1 > 0$ from this interval we have that

$$\begin{aligned} \frac{\partial G_1}{\partial C_1} &= \mu_1 \Bigg[-\frac{\alpha_1 K_1^1}{((K_1^1 + P_{tot}) - \alpha_1 C_1)^2} \frac{(N_{tot} - \beta_1 C_1)}{((K_2^1 + N_{tot}) - \beta_1 C_1)} \\ &\quad - \frac{(P_{tot} - \alpha_1 C_1)}{((K_1^1 + P_{tot}) - \alpha_1 C_1)} \frac{\beta_1 K_2^1}{((K_2^1 + N_{tot}) - \beta_1 C_1)^2} \Bigg] < 0, \end{aligned} \tag{26}$$

which means that $G_1(C_1, 0)$ is a decreasing function of C_1.

Condition (24) states that $G_1(0,0) > 0$; relation (26) shows that the function is monotonously decaying as C_1 is increasing; finally, $G_1(C_1, 0) < 0$ when $C_1 = \min[P_{tot}/\alpha_1, N_{tot}/\beta_1]$. Thus, there exists a unique $\bar{C}_1 = C_1^* \in (0, \min[P_{tot}/\alpha_1, N_{tot}/\beta_1])$ where $G_1(C_1^*, 0) = 0$. For this value of $\bar{C}_1 = C_1^* > 0$, due to (26), the first stability condition, on λ_1, in (23) is satisfied. Condition (25) guarantees that there is no other non-trivial steady states. So, when the non-trivial steady state $(C_1^*, 0)$ exists (and there are no other non-trivial steady states) it is also stable.

Similarly, for the existence and stability of the unique non-trivial steady state $(\bar{C}_1, \bar{C}_2) = (0, C_2^*)$ we must have $G_1(0,0) < 0$ and $G_2(0,0) > 0$. The value of $C_2 = C_2^*$ is found as a solution of $G_2(0, C_2) = 0$.

The co-existence of the two mentioned above non-trivial steady states (and possibility of a steady state $(\bar{C}_1, \bar{C}_2) = (C_1^{**}, C_2^{**})$, where both species concentrations are positive: $C_1^{**} > 0$, $C_2^{**} > 0$) is observed when both $G_1(0,0) > 0$ and $G_2(0,0) > 0$.

In Appendix B we show that for non-degenerate cases the null-clines

$$G_1(C_1, C_2) = 0 \quad \text{and} \quad G_2(C_1, C_2) = 0 \tag{27}$$

may have at most one intersection in the first quadrant. Also, it can be easily seen from (15) that each equation,

$$G_1(C_1, 0) = 0, \quad G_2(0, C_2) = 0, \quad G_1(0, C_2) = 0, \quad G_2(C_1, 0) = 0,$$

has a unique positive root if $G_1(0,0) > 0$ and $G_2(0,0) > 0$ (the argument is similar to that presented earlier). Then, the analysis of stability of these co-existing steady states follows closely a similar analysis for a classical competition model (where null-clines are straight lines, and for which the *principle of competitive exclusion* is naturally established).

Let us denote solutions of $G_1(C_1, 0) = 0$ and $G_2(0, C_2) = 0$ by $C_1 = C_1^*$ and $C_2 = C_2^*$, respectively, and solutions of $G_1(0, C_2) = 0$ and $G_2(C_1, 0) = 0$ by $C_2 = \hat{C}_2$ and $C_1 = \hat{C}_1$, respectively. We note that $(C_1^*, 0)$ and $(0, C_2^*)$ are the steady states, while $(\hat{C}_1, 0)$ and $(0, \hat{C}_2)$ are not!

Each null-cline $G_i(C_1, C_2) = 0$ $(i = 1, 2)$ separates the first quadrant into a pair of domains. In each of these domains $G_i(C_1, C_2)$ maintains its sign, i.e., in the domain that includes the origin, (0,0), $G_i(C_1, C_2) > 0$, while in the complementary domain $G_i(C_1, C_2) < 0$. The following four possibilities may take place (we exclude from consideration degenerate cases for which $C_1^* = \hat{C}_1$ or $C_2^* = \hat{C}_2$):

$$C_1^* > \hat{C}_1, \qquad C_2^* < \hat{C}_2; \tag{28}$$

$$C_1^* < \hat{C}_1, \qquad C_2^* > \hat{C}_2; \tag{29}$$

$$C_1^* > \hat{C}_1, \qquad C_2^* > \hat{C}_2; \tag{30}$$

$$C_1^* < \hat{C}_1, \qquad C_2^* < \hat{C}_2; \tag{31}$$

A simple analysis of the behavior of velocity vector fields on the (C_1, C_2)-phase plane for each of the above mentioned cases allows us to make the following conclusions.

For the case of conditions (28), the steady state $(C_1^*, 0)$ is stable (node) and the steady state $(0, C_2^*)$ is unstable (saddle). A steady state where both species have non-trivial populations does not exist in this case since under conditions (28), if one intersection of null-clines takes place, then the second one must also be observed, which is impossible due to the fact that when such intersection does exist, it must be unique (see discussion presented in Appendix B).

When conditions (29) are satisfied, the steady state $(0, C_2^*)$ is stable (node) and the steady state $(C_1^*, 0)$ is unstable (saddle). Same as in the previous case, a steady state where both species have non-trivial populations does not exist for the case of conditions (29).

Under conditions (30), both steady states, $(C_1^*, 0)$ and $(0, C_2^*)$, are stable (nodes). In this case the null-clines (27) intersect (at exactly one point; see Appendix B). This intersection corresponds to a unique steady state for which both species have non-zero concentrations. Analysis of velocity vector field in the vicinity of the null-clines intersection point shows that this steady state is unstable (saddle).

Finally, when conditions (31) are satisfied, both steady states, $(C_1^*, 0)$ and $(0, C_2^*)$, are unstable (sadles). In this case the null-clines (27) also intersect (at exactly one point; see Appendix B). This intersection, a unique steady state for which both species have non-zero concentrations, is now a stable node.

In the above discussion we referred to the fact that if the null-clines intersect in the first quadrant, then they only intersect once. Unlike classical competition model with linear null-clines, here the null-clines are not linear, so, in principle they may have more than one intersection in the first quadrant. In Appendix B we show that this is not the case, i.e., that when it exists, the null-clines intersection point in the first quadrant, and thus, the non-trivial populations co-existence steady state, is unique.

Appendix B. Uniqueness of a steady state for which both species have non-trivial population concentrations

Next, we discuss a constructive approach to finding a steady state $(\bar{C}_1, \bar{C}_2) = (C_1^{**}, C_2^{**})$ for which $C_1 = C_1^{**} > 0$ and $C_2 = C_2^{**} > 0$.

It follows from (16) that non-trivial $(C_1, C_2) = (\bar{C}_1, \bar{C}_2)$ can be found as a simultaneous solution (if it exists) of the equations:

$$G_1(C_1, C_2) = 0, \qquad G_1(C_1, C_2) = 0. \tag{32}$$

The above system for convenience may be re-written as

$$\begin{aligned} \frac{X}{(K_1^1 + X)} \frac{Y}{(K_2^1 + Y)} &= \frac{M_1}{\mu_1} = \tilde{M}_1, \\ \frac{X}{(K_1^2 + X)} \frac{Y}{(K_2^2 + Y)} &= \frac{M_2}{\mu_2} = \tilde{M}_2; \end{aligned} \tag{33}$$

where

$$\begin{aligned} P_{tot} - \alpha_1 C_1 - \alpha_2 C_2 &= X, \\ N_{tot} - \beta_1 C_1 - \beta_2 C_2 &= Y. \end{aligned} \tag{34}$$

It follows from (33), (34) that the corresponding solution can be found in two steps: first, we solve (33) for X and Y, and then, find $C_1 = \bar{C}_1$, $C_2 = \bar{C}_2$ from (34) that, in turn, can be written as

$$\begin{aligned} \alpha_1 C_1 + \alpha_2 C_2 &= P_{tot} - X, \\ \beta_1 C_1 + \beta_2 C_2 &= N_{tot} - Y. \end{aligned} \tag{35}$$

One of the conditions for unique solvability of (35) (equivalent to (34)) is that the matrix

$$H = \begin{pmatrix} \alpha_1 & \alpha_2 \\ \\ \beta_1 & \beta_2 \end{pmatrix} \tag{36}$$

is non-singular. This means that we must have:

$$\det H = \alpha_1\beta_2 - \alpha_2\beta_1 \neq 0. \tag{37}$$

Also, to obtain biologically meaningful solution (population densities are non-negative), we require to only consider such X and Y that $(P_{tot} - X) > 0$ and $(N_{tot} - Y) > 0$.

Next, let us concentrate on the analysis of (33). The non-trivial solution satisfying $0 < X = X^* < P_{tot}$, $0 < Y = Y^* < N_{tot}$ (which is of interest to us), can geometrically be represented as an intersection of the two curves (hyperbolas) described by the functions that are obtained from (33):

$$\begin{aligned} X &= \frac{K_1^1\tilde{M}_1(K_2^1 + Y)}{(1-\tilde{M}_1)Y - K_2^1\tilde{M}_1} =: L_1(Y), \\ X &= \frac{K_1^2\tilde{M}_2(K_2^2 + Y)}{(1-\tilde{M}_2)Y - K_2^2\tilde{M}_2} =: L_2(Y). \end{aligned} \tag{38}$$

Then, Y^* satisfies $L_1(Y^*) = L_2(Y^*)$, while $X^* = L_1(Y^*)$, or $X^* = L_2(Y^*)$.

We note that for the solutions X, Y of (33) (that produce biologically meaningful C_1, C_2) to exist, certain constraints must be imposed on coefficients: i.e., we must require that

$$0 < \tilde{M}_1 < 1, \qquad 0 < \tilde{M}_2 < 1. \tag{39}$$

This, in turn, means that coefficients multiplying Y in the denominators of the right-hand sides of equations (38) will satisfy $(1 - \tilde{M}_i) > 0$.

Let us show why we can only have at most one solution of (33) for which both $X = X^* > 0$ and $Y = Y^* > 0$.

First, we note that it follows from (38) that to have $X = X^* > 0$ the value of $Y = Y^* > 0$ must satisfy the inequality:

$$Y^* > \max\left(\frac{K_2^1\tilde{M}_1}{(1-\tilde{M}_1)}, \frac{K_2^2\tilde{M}_2}{(1-\tilde{M}_2)}\right). \tag{40}$$

Eliminating X from (38), we can write

$$K_1^1\tilde{M}_1(K_2^1 + Y)((1-\tilde{M}_2)Y - K_2^2\tilde{M}_2) = K_1^2\tilde{M}_2(K_2^2 + Y)((1-\tilde{M}_1)Y - K_2^1\tilde{M}_1). \tag{41}$$

Geometrically, possible solutions of (41) now correspond to intersection of two parabolas. Quadratic function on the left hand side of (41) has 2 roots: $Y_L^1 = -K_2^1 < 0$,

$Y_L^2 = K_2^2\tilde{M}_2/(1-\tilde{M}_2) > 0$; and quadratic function on the right hand side of (41) has 2 roots: $Y_R^1 = -K_2^2 < 0$, $Y_R^2 = K_2^1\tilde{M}_1/(1-\tilde{M}_1) > 0$.

From condition (40) it follows that biologically meaningful value of Y^* must lie to the right of both, Y_L^2 and Y_R^2. For $Y > \max(Y_L^2, Y_R^2)$ the parabolas described by the functions in the left and in the right hand sides of (41) will be increasing. Assume that we have one Y^* satisfying condition (40). At this point of intersection the slopes of the parabolas are different. Assume that the slopes satisfy the inequality $K_1^1\tilde{M}_1(1-\tilde{M}_2)Y^* > K_1^2\tilde{M}_2(1-\tilde{M}_1)Y^*$ (or $K_1^1\tilde{M}_1(1-\tilde{M}_2)Y^* < K_1^2\tilde{M}_2(1-\tilde{M}_1)Y^*$). Then the same inequality will be satisfied for all $Y > Y^*$. However, for an additional solution of (41) satisfying the condition (40) to exist, we must have the situation where mentioned above inequality for slopes changes sign for some $Y > Y^*$. Since this is not possible, there is no second biologically meaningful solution of (41).

To actually find the non-trivial steady state solutions, let us re-write equation (41) for $Y = Y^*$ in the form

$$\begin{gathered}[K_1^1\tilde{M}_1(1-\tilde{M}_2) - K_1^2\tilde{M}_2(1-\tilde{M}_1)]Y^2 \\ +[K_1^1\tilde{M}_1K_2^1(1-\tilde{M}_2) - K_1^2\tilde{M}_2K_2^2(1-\tilde{M}_1)]Y \\ -[K_1^1\tilde{M}_1K_2^2\tilde{M}_2 - K_1^2\tilde{M}_2K_2^1\tilde{M}_1]Y \\ -[K_1^1\tilde{M}_1K_2^1\tilde{M}_2K_2^2 - K_1^2\tilde{M}_2K_2^2\tilde{M}_1K_2^1] = 0.\end{gathered} \tag{42}$$

We introduce the following notation:

$$\begin{gathered}A = [K_1^1\tilde{M}_1(1-\tilde{M}_2) - K_1^2\tilde{M}_2(1-\tilde{M}_1)]; \\ B = [K_1^1\tilde{M}_1K_2^1(1-\tilde{M}_2) - K_1^2\tilde{M}_2K_2^2(1-\tilde{M}_1)] \\ -[K_1^1\tilde{M}_1K_2^2\tilde{M}_2 - K_1^2\tilde{M}_2K_2^1\tilde{M}_1]; \\ D = -[K_1^1\tilde{M}_1K_2^1\tilde{M}_2K_2^2 - K_1^2\tilde{M}_2K_2^2\tilde{M}_1K_2^1].\end{gathered}$$

The biologically meaningful solution that we seek is then given by

$$Y^* = \frac{-B + \sqrt{B^2 - 4AD}}{2A}, \tag{43}$$

when it exists (i.e., it is real and positive), with $X^* = L_1(Y^*) = L_2(Y^*)$.

Finally,

$$\begin{pmatrix} C_1^{**} \\ \\ C_2^{**} \end{pmatrix} = H^{-1} \begin{pmatrix} P_{tot} - X^* \\ \\ N_{tot} - Y^* \end{pmatrix}. \tag{44}$$

The stability properties of this equilibrium point $(\bar{C}_1, \bar{C}_2) = (C_1^{**}, C_2^{**})$ were discussed in Appendix A.